

DESY 96-179

DIFFRACTIVE INTERACTIONS

V. DEL DUCA

*Particle Physics Theory Group, Dept. of Physics and Astronomy
University of Edinburgh, Edinburgh EH9 3JZ, Scotland, UK*

E. GALLO

INFN Firenze, Largo E. Fermi 2, 50125 Firenze, Italy

P. MARAGE

Université Libre de Bruxelles, Bd. du Triomphe, B-1050 Brussels, Belgium

The general framework of diffractive deep inelastic scattering is introduced and reports given in the session on diffractive interactions at the International Workshop on Deep-Inelastic Scattering and Related Phenomena, Rome, April 1996, are presented.

1 Introduction

Since the first observations of large rapidity gap events in deep-inelastic scattering at HERA^{1,2}, diffractive interactions have attracted much attention. In this Conference, 31 reports (about half theoretical and half experimental) have been presented to the working group on diffraction, of which 15 were presented in sessions held in common with the working groups on structure functions, on photoproduction and on final states. Two discussion sessions were devoted mainly to the interpretation of the inclusive measurements. Reports were also presented on the DESY Workshop on the future of HERA³, and on Monte Carlo simulations of diffractive processes⁴. The experimental results concern mainly HERA, but also experiments at the Tevatron collider. The present summary consists of two parts, devoted respectively to inclusive measurements^a and to exclusive vector meson production^b.

2 DDIS Inclusive Measurements*2.1 Introduction*

Diffractive interactions, sketched in Fig. 1, are attributed to the exchange of a colour singlet system, the pomeron, and are characterised by the presence in

^apresented by V. Del Duca and P. Marage

^bpresented by E. Gallo

the final state of a large rapidity gap, without particle emission, between two systems X and Y of masses M_X and M_Y much smaller than the total hadronic mass W . The final state system Y is a proton (elastic scattering) or an excited state of higher mass (proton dissociation).

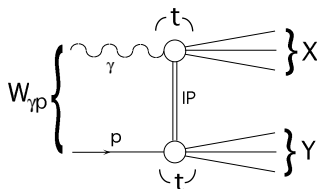


Figure 1: Diffractive interaction in photo- or electroproduction $\gamma^{(*)}p \rightarrow XY$.

The cross section for diffractive deep inelastic scattering (DDIS) is defined using four variables (in addition to the mass M_Y of the system Y), *e.g.* Q^2 (the negative four-momentum squared of the exchanged photon), the Bjorken scaling variable x , the total hadronic mass W , and the square of the pomeron four-momentum t . It is also useful to define the variables x_P and β

$$x_P = \frac{Q^2 + M_X^2 - t}{Q^2 + W^2 - M_p^2}, \quad \beta = \frac{Q^2}{Q^2 + M_X^2 - t}, \quad (1)$$

which are related to x by the relation $x = \beta \cdot x_P$.

Inclusive DIS is usually parameterised in terms of two structure functions, $F_i = F_i(x, Q^2)$, with $i = 1, 2$. DDIS needs in principle four structure functions, which can be written in such a way that two are similar to the ones of inclusive DIS, and the other two are the coefficients of terms proportional to the t variable, and may be neglected since t is small⁵. Thus, in analogy with inclusive DIS the cross section for DDIS is written as

$$\frac{d^4\sigma(e + p \rightarrow e + X + Y)}{dx dQ^2 dx_P dt} = \frac{4\pi\alpha^2}{xQ^4} \left[1 - y + \frac{y^2}{2(1 + R^D)} \right] F_2^{D(4)}(x, Q^2; x_P, t), \quad (2)$$

with $y = Q^2/x \cdot s$ the electron energy loss, s the total (e, p) centre of mass energy, and

$$R^D(x, Q^2; x_P, t) = \frac{1}{2x} \frac{F_2^{D(4)}}{F_1^{D(4)}} - 1. \quad (3)$$

R has not been measured yet in the inclusive DIS, and R^D will be set to 0 in what follows. Therefore the diffractive cross section (2) is directly related to

$F_2^{D(4)}$ ^c. If factorization of the collinear singularities works in this case as it does in inclusive DIS, then the diffractive structure function may be written in terms of a parton density of the pomeron ⁶,

$$F_2^{D(4)}(x, Q^2; x_P, t) = \sum_a \int_x^{x_P} d\zeta \frac{df_{a/p}^D(\zeta, \mu; x_P, t)}{dx_P dt} \hat{F}_{2,a} \left(\frac{x}{\zeta}, Q^2, \mu \right), \quad (4)$$

with ζ the parton momentum fraction within the proton, x_P the momentum fraction of the pomeron, μ the factorization scale, and the sum extending over quarks and gluons; the parton structure functions $\hat{F}_{2,a}$ are computable in perturbative QCD. The integral of the diffractive parton density over t is the fracture function ⁷

$$\int_{-\infty}^0 dt \frac{df_{a/p}^D(\zeta, \mu; x_P, t)}{dx_P dt} = M_{pp}^a(\zeta, \mu; x_P). \quad (5)$$

The structure function $F_2^{D(3)}$ is obtained by integration of $F_2^{D(4)}$ over the t variable. It is thus related to the fracture function by

$$F_2^{D(3)}(x, Q^2; x_P) = \sum_a \int_x^{x_P} d\zeta M_{pp}^a(\zeta, \mu; x_P) \hat{F}_{2,a} \left(\frac{x}{\zeta}, Q^2, \mu \right). \quad (6)$$

Next, let us assume that Regge factorization holds for the diffractive parton density, namely that it can be factorized into a flux of pomeron within the proton and a parton density within the pomeron ^{8,9}:

$$\frac{df_{a/p}^D(\zeta, \mu; x_P, t)}{dx_P dt} = \frac{f_{pP}(x_P, t)}{x_P} f_{a/P} \left(\frac{\zeta}{x_P}, \mu; t \right), \quad (7)$$

with flux

$$f_{pP}(x_P, t) = \frac{|\beta_{pP}(t)|^2}{8\pi^2} x_P^{1-2\alpha(t)}, \quad (8)$$

the pomeron-proton coupling $\beta_{pP}(t)$ and the trajectory $\alpha(t)$ ^d being obtained from fits to elastic hadron-hadron cross sections at small t ^{5,10},

$$\begin{aligned} \beta_{pP}(t) &= \beta_{\bar{p}P}(t) \simeq 4.6 \text{ mb}^{1/2} e^{1.9 \text{ GeV}^{-2} t}, \\ \alpha(t) &\simeq 1.08 + 0.25 \text{ GeV}^{-2} t. \end{aligned} \quad (9)$$

^cIn the theoretical literature the diffractive structure function $F_2^{D(4)}$ is often called $\frac{dF_2^D}{dx_P dt}$.

^dFor simplicity the trajectory is supposed to be linear ¹⁰, however it is also possible to consider models with a non-linear trajectory ¹¹.

Substituting the diffractive parton density (7) into the structure function (4), we obtain

$$F_2^{D(4)}(x, Q^2; x_P, t) = f_{pP}(x_P, t) F_2^P(\beta, Q^2; t), \quad (10)$$

with the pomeron structure function

$$F_2^P(\beta, Q^2; t) = \sum_a \int_\beta^1 d\beta' f_{a/P}(\beta', \mu; t) \hat{F}_{2,a}\left(\frac{\beta}{\beta'}, Q^2, \mu\right), \quad (11)$$

with $\beta' = \zeta/x_P$ and β the fraction of the pomeron momentum carried by the struck parton. When the outgoing proton momentum is measured as the fraction x_L of the incident proton momentum, one has $x_L \simeq 1 - x_P$.

Several reports at this Conference and numerous discussions dealt with the procedures of diffractive cross section measurement, the factorisation properties of the structure function and the possibility to extract parton distributions for the exchange system.

2.2 Cross section measurements

The H1¹² and ZEUS¹³ experiments have measured the cross section for diffractive deep inelastic scattering in the data taken in 1993, by selecting events with a large rapidity gap in the forward part of their main calorimeters. The non-diffractive and the proton dissociation diffractive contributions were subtracted using Monte Carlo simulations. Within the limited statistics, both experiments found that the results were compatible with a factorisation of the structure function $F_2^{D(3)}$ of the form

$$F_2^{D(3)}(Q^2, \beta, x_P) = \frac{1}{x_P^n} A(Q^2, \beta), \quad (12)$$

where the x_P dependence could be interpreted as proportional to a pomeron flux in the proton, in agreement with eq. (10) integrated over t . The exponent n is related to the effective pomeron trajectory by $n = 2\alpha(t) - 1$, as in eq. (8), with $\alpha(t)$ given in eq. (9).

The following t averaged $\bar{\alpha}$ values were obtained by H1 and ZEUS, respectively:

$$\bar{\alpha} = 1.10 \pm 0.03 \pm 0.04 \quad \text{H1} \quad (13)$$

$$\bar{\alpha} = 1.15 \pm 0.04 \begin{smallmatrix} +0.04 \\ -0.07 \end{smallmatrix} \quad \text{ZEUS.} \quad (14)$$

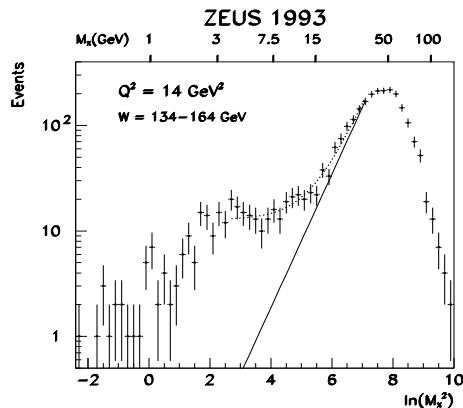


Figure 2: ZEUS Coll. ($\log M_X$ method [14]): Example of a fit for the determination of the nondiffractive background. The solid lines show the extrapolation of the nondiffractive background as determined from the fit of the diffractive and nondiffractive components to the data (dotted line).

The ZEUS Collaboration has presented at this Conference a different method to extract the diffractive contribution (1993 data)¹⁴. The (uncorrected) $\log M_X^2$ distributions, in bins of Q^2 and W , are parameterised as the sum of an exponentially falling contribution at high M_X , attributed to non-diffractive interactions, and of a constant contribution at low M_X , attributed to diffraction. (see Fig. 2). With this “operational definition” of diffraction (with $M_Y \lesssim 4 \text{ GeV}/c^2$), no Monte Carlo simulations are used. The W dependence of the diffractive cross section gives (see Fig. 3):

$$\bar{\alpha} = 1.23 \pm 0.02 \pm 0.04, \quad \beta = 0.1 - 0.8. \quad (15)$$

The difference with the previously published result is attributed by ZEUS to the uncertainties in the Monte Carlo procedure for background subtraction.

The ZEUS Collaboration has also presented in this Conference preliminary results obtained with the Leading Proton Spectrometer (1994 data)¹⁵. In this case, the scattered proton is unambiguously tagged, and the kinematics are reconstructed using its momentum measurement. A fit of the $x_{\mathbb{P}}$ dependence (see Fig. 4) for $\langle M_X^2 \rangle = 100 \text{ GeV}^2$ gives:

$$\bar{\alpha} = 1.14 \pm 0.04 \pm 0.08, \quad \beta = 0.04 - 0.5. \quad (16)$$

The ZEUS LPS has also provided the first inclusive measurement of the

ZEUS 1993

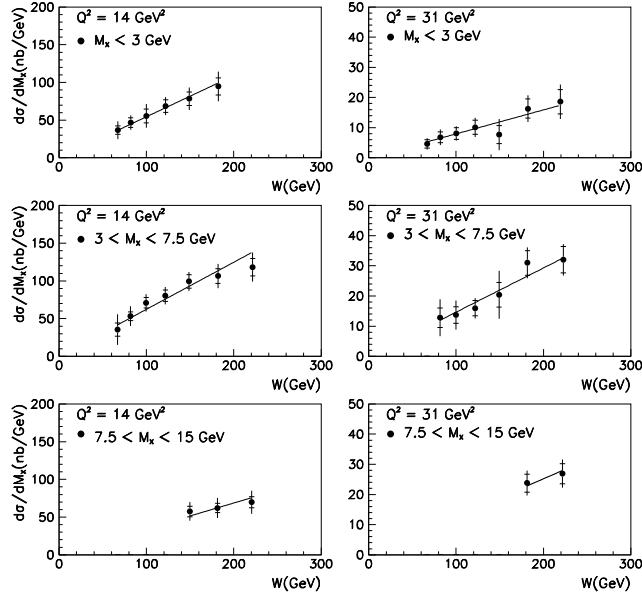


Figure 3: ZEUS Coll. ($\log M_X$ method [14]): The differential cross sections $d\sigma^{diff}(\gamma^*p \rightarrow XN)/dM_X$. The inner error bars show the statistical errors and the full bars the statistical and systematic errors added in quadrature. The curves show the results from fitting all cross sections to the form $d\sigma^{diff}/dM_X \propto (W^2)^{(2\overline{\alpha_{IP}}-2)}$ with a common value of $\overline{\alpha_{IP}}$.

ZEUS 94 PRELIMINARY

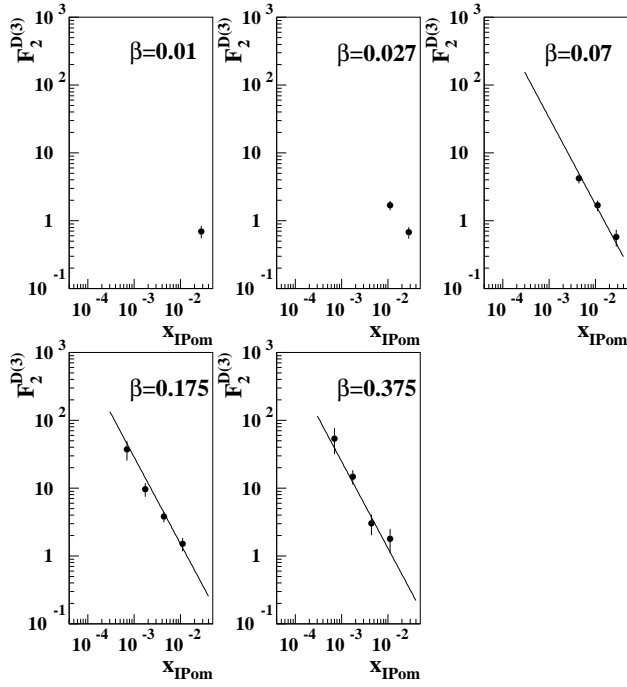


Figure 4: ZEUS Coll. (LPS data [15]): The structure function $F_2^{D(3)}$, plotted as a function of x_{IP} in 5 bins in β at a central value $Q^2 = 12 \text{ GeV}^2$. The errors are statistical only. The solid line corresponds to a fit in the form of eq. (12).

diffractive t dependence at HERA, parameterised as

$$\frac{d\sigma}{dt} \propto e^{-b|t|}, \quad b = 5.9 \pm 1.3^{+1.1}_{-0.7} \text{ GeV}^{-2}. \quad (17)$$

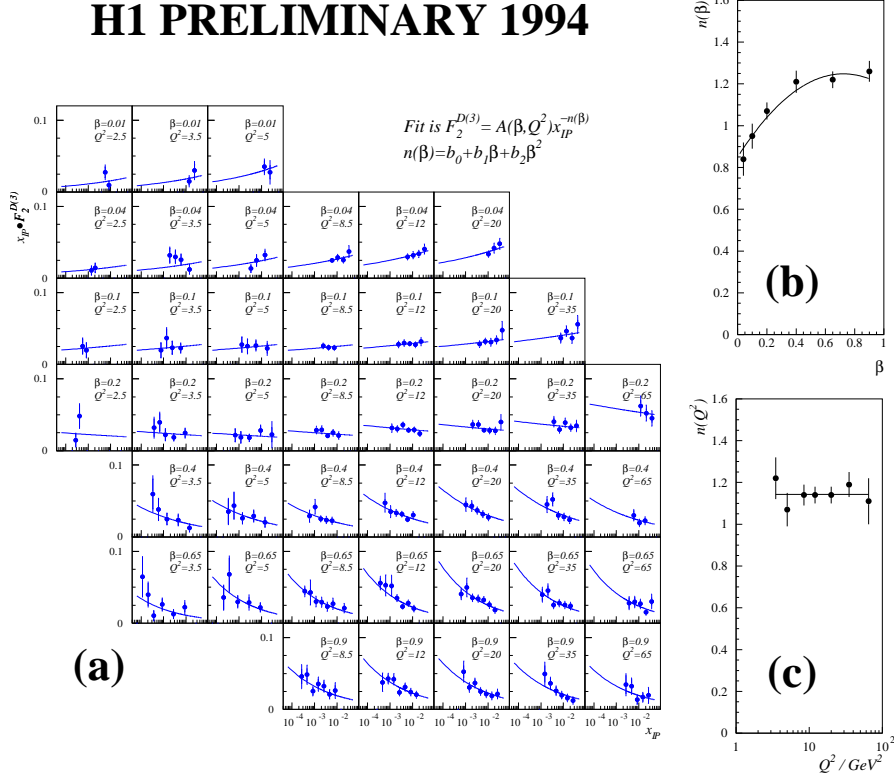


Figure 5: H1 Coll. [16]: (a) $x_{\mathbb{P}} \cdot F_2^{D(3)}(\beta, Q^2, x_{\mathbb{P}})$ integrated over the range $M_Y < 1.6$ GeV and $|t| < 1$ GeV²; (b) the β dependence of n when $F_2^{D(3)}$ is fitted to the form $F_2^{D(3)} = A(\beta, Q^2)/x_{\mathbb{P}}^{n(\beta)}$; (c) the Q^2 dependence of n when $F_2^{D(3)}$ is fitted to the form $F_2^{D(3)} = A(\beta, Q^2)/x_{\mathbb{P}}^{n(Q^2)}$. The experimental errors are statistical and systematic added in quadrature.

Finally, the H1 Collaboration has reported preliminary results on $F_2^{D(3)}$ from the 1994 data¹⁶. The use of the forward detectors allows the selection of events with no activity in the pseudorapidity range $3.2 < \eta < 7.5$ ($M_Y < 1.6$ GeV/c²). With this extended kinematical domain and a tenfold increase in

statistics compared to the 1993 data, 43 bins in Q^2 and β are defined. A clear breaking of factorisation is observed: in the form of parameterisation (12), the data suggest that the n exponent is independent of Q^2 but they require a definite β dependence, with $\bar{\alpha}$ ranging from $\simeq 0.98$ for $\langle\beta\rangle \simeq 0.1$ to $\simeq 1.12$ for $\langle\beta\rangle \gtrsim 0.4$ (see Fig. 5).

Experimentally, for similar values of $\langle\beta\rangle$, the H1 results thus favour a smaller value of $\bar{\alpha}$ than the $(\log M_X^2)$ ZEUS analysis. Detailed comparisons and discussions between the two experiments should in the future provide more information concerning the source of this difference.

2.3 Factorisation Breaking and Parton Distributions

The source of the factorisation breaking observed by H1 has been discussed in several communications and during the round tables.

N. N. Nikolaev underlined particularly that the pomeron is not a particle, and that in a QCD inspired approach, factorisation is not expected to hold¹⁷.

The possible contribution in the selected samples of different exchanges, in particular of pomeron and f and a_2 trajectories, was particularly emphasised^{11,17,18,19,20,21}. These trajectories have different energy and thus $x_{\mathbb{P}}^n$ dependences. They have also different partonic contents, and thus different functions $A(Q^2, \beta)$ describe the interaction with the photon. Even if each contribution were factorisable, their combination would thus not be expected to allow a factorisable effective parameterisation.

However, if it is possible to select a domain where pomeron exchange dominates, and if the factorization picture outlined in sect. 2.1 holds, it is possible to fit the data on single hard diffraction to extract the parton densities in the pomeron^e. First we note that the pomeron, being an object with the quantum numbers of the vacuum, has $C = 1$ and is isoscalar^{10 f}. The former property implies that $f_{q/\mathbb{P}}(\beta) = f_{\bar{q}/\mathbb{P}}(\beta)$ for any quark q and the latter that $f_{u/\mathbb{P}}(\beta) = f_{d/\mathbb{P}}(\beta)$. Therefore it is necessary to determine only the up and strange quark densities and the gluon density. Since the parton structure function is,

$$\hat{F}_{2,a}\left(\frac{\beta}{\beta'}, Q^2, \mu\right) = e_a^2 \delta\left(1 - \frac{\beta}{\beta'}\right) + O(\alpha_s), \quad (18)$$

with e_a the quark charge and a running over the quark flavors, the pomeron

^eIt is not clear whether the fits should be extended to data from hadron-hadron scattering or from photoproduction because of additional factorization-breaking contributions²².

^fA $C = -1$ contribution would be indication of an odderon exchange²⁰.

structure function (11) becomes,

$$F_2^{\mathcal{P}}(\beta, Q^2; t) = \frac{10}{9}\beta f_{u/\mathcal{P}}(\beta, Q^2; t) + \frac{2}{9}\beta f_{s/\mathcal{P}}(\beta, Q^2; t) + O(\alpha_s), \quad (19)$$

where the gluon density contributes to the $O(\alpha_s)$ term through the DGLAP evolution.

H1 PRELIMINARY 1994

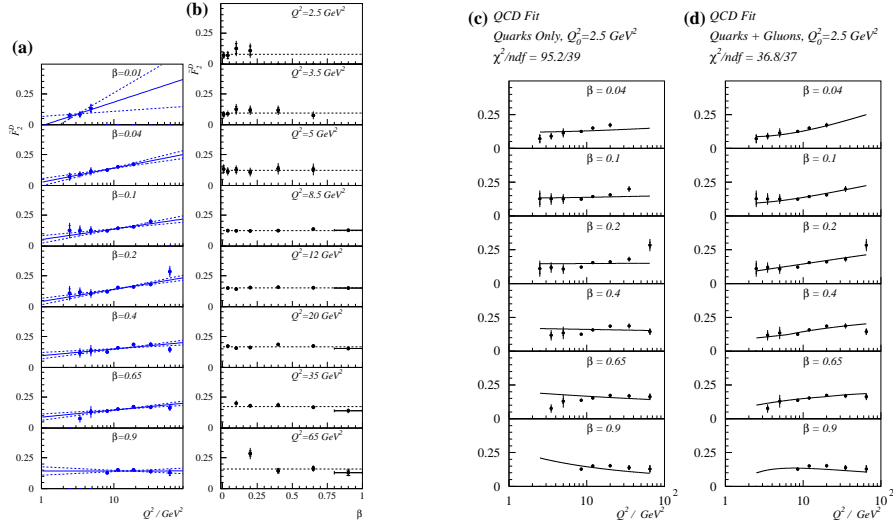


Figure 6: H1 Coll. [16]: (a) $\tilde{F}_2^D(\beta, Q^2)$ as a function of Q^2 for different β values. The superimposed lines correspond to the best fit to a linear dependence on $\ln Q^2$ (continuous) and $\pm 1\sigma$ (dashed); (b) $\tilde{F}_2^D(\beta, Q^2)$ as a function of β for different Q^2 values, with a best fit to a constant β dependence; (c) DGLAP QCD comparison of the (β, Q^2) dependence of \tilde{F}_2^D assuming only quarks at the starting scale of $Q_0^2 = 2.5 \text{ GeV}^2$; (d) DGLAP QCD comparison of the (β, Q^2) dependence of \tilde{F}_2^D assuming both quarks and gluons at the starting scale.

The H1 Collaboration has studied the evolution of the structure function $F_2^{D(3)}$, integrated over $x_{\mathcal{P}}$ in the range $0.0003 < x_{\mathcal{P}} < 0.05$ (in practice, most of the data are for $x_{\mathcal{P}} < 0.02$):

$$\tilde{F}_2^D(Q^2, \beta) = \int F_2^{D(3)}(Q^2, \beta, x_{\mathcal{P}}) dx_{\mathcal{P}}. \quad (20)$$

It is observed (see Fig. 6) that $\tilde{F}_2^D(Q^2, \beta)$ shows no β dependence at fixed Q^2 but increases with Q^2 for fixed β values, up to large β . If interpreted in

a partonic framework, this behaviour, strikingly different of that of ordinary hadrons, is suggestive of an important gluonic contribution at large β .

More specifically, the H1 Collaboration assumed the possibility to perform a QCD analysis of this evolution of \tilde{F}_2^D using the DGLAP equations (with no inhomogeneous term) to extract parton densities in the exchange. At $Q^2 = 5 \text{ GeV}^2$, a leading gluon component is obtained. When the corresponding parton densities are input in Monte Carlo simulations of exclusive processes (sect. 2.4), consistent results are obtained^{23,24,25}.

This procedure was discussed during the round tables and in several contributions. In the absence of factorisation theorems (see²⁶), it can be questioned whether the parton distribution functions are universal, and whether they obey a DGLAP evolution. A specific problem, due to the fact that the pomeron is not a particle, is that momentum sum rules need not be valid. However, it was noticed that the contribution of several Regge trajectories may not affect the validity of a common QCD-DGLAP evolution, in so far as these exchanges can all be given a partonic interpretation²¹.

On the other hand, it was also argued^{17,27} that, even if one accepts the concept of parton density functions in the diffractive exchange, the DGLAP evolution should not be valid at high β , because of charm threshold effects and because of the specific and different Q^2 evolutions of the longitudinal and transverse contributions.

2.4 Parton Distributions and Jet Production

Jet production in diffractive interactions has yielded the first hint of a partonic structure of the pomeron⁸. We have seen in sect. 2.3 how the quark densities may be directly related to the pomeron structure function. The gluon density may also be directly measured by using data on diffractive charm or jet production. For the latter, the final state of the hard scattering $jet_1 + jet_2 + X$ consists at the lowest order $O(\alpha_s)$ of two partons only, generated in quark-exchange and Compton-scattering diagrams for quark-initiated hard processes, and in photon-gluon fusion diagrams for the gluon-initiated ones. The parton momentum fraction x in the proton may be computed from the jet kinematic variables, $x = (E/P^0) \exp(2\bar{\eta})$, with E and P^0 the electron and proton energies and $\bar{\eta} = (\eta_{j_1} + \eta_{j_2})/2$ the rapidity boost of the jet system. The momentum fraction x_P may be obtained from the invariant mass of the system recoiling against the proton, $x_P \simeq M_{e j_1 j_2}^2/s$. If we neglect the strange quark density⁹, the data on F_2^D and diffractive jet production suffice to measure the parton

⁹The strange quark density might be measured adding to the fit data on charged-current charm production in DDIS⁵.

densities in the pomeron, and may be used to link the value of the momentum sum, $\sum_a \int_0^1 dx x f_{a/P}(x)$, to the gluon content of the pomeron²⁸.

On the other hand, if the gluon density is determined from F_2^D alone, as outlined in sect. 2.3, one can make predictions for the data on diffractive charm or jet production. Indeed, using the data on F_2^D and the Monte Carlo RAPGAP²⁹, based on the factorization (10), the H1 Collaboration¹⁶ finds that the parton densities $f_{a/P}$ are dominated by a very hard gluon^h (sect. 2.3). Having measured the densities $f_{a/P}$, the H1 Collaboration²³ finds that the jet rapidity and transverse momentum distributions in diffractive dijet production are in good agreement with the prediction from RAPGAP. In addition, the data on energy flow in diffractive photoproduction also seem to support a gluon-dominated structure of the pomeron²⁴.

Besides, by examining the thrust we may probe the amount of gluon radiation in diffractive dijet production. The thrust axis is defined as the axis in the parton center-of-mass system along which the energy flow is maximal. The value of the thrust, T , then measures the fraction of energy along this axis. For a back-to-back dijet event $T = 1$; so the amount by which T differs from unity gives an indication on the amount of emitted gluon radiation. The data²⁵ shows indeed the presence of hard gluon radiation, the thrust being even smaller than in dijet production in e^+e^- annihilation.

Finally, we mention several angular-correlation analyses recently proposed. Namely, the azimuthal-angle distribution in diffractive dijet production²⁷; the final-state electron-proton azimuthal-angle distribution in the lab frame³¹; the azimuthal-angle distribution of the initial electron in the photon-proton frame³². The respective measurements, if carried out, should allow to further probe the pomeron structure, and to discriminate between different models.

2.5 Other Measurements

In addition to these diffractive DIS measurements, the HERA Collaborations also contributed reports on several other topics.

The H1 Collaboration presented results on diffraction in photoproduction¹⁶, with a measurement of its decomposition in vector meson production, photon dissociation, proton dissociation and double dissociation. In particular, the M_X distribution is consistent with soft pomeron exchange.

The ZEUS experiment reported the observation of a charged current diffractive candidate event in the 1994 data³³, and discussed the design of a special trigger used in the 1995 data taking.

^hThere are models^{22,30} which predicted the dominance of a single hard gluon. In these models the color is neutralized by the exchange of one or more soft gluons.

ZEUS also presented the observation of DIS events with a high energy neutron produced at very small angle with respect to the proton direction, detected in their neutron counter³⁴. These events, attributed to pion exchange, account for about 10% of the total DIS rate, independent of x and Q^2 .

Finally, the E665 muon experiment at Fermilab reported on the ratio of diffractive to inelastic scattering³⁵.

3 Exclusive Vector Meson Production

3.1 Introduction

Exclusive vector mesons production at HERAⁱ is a very interesting process to study the transition from a non-perturbative description of the pomeron, the 'soft' pomeron, to the hard perturbative pomeron.

The process that we study is shown in figure 7a and corresponds to the reaction

$$ep \rightarrow eVN, \quad (21)$$

where V is a vector meson ($\rho, \omega, \phi, \rho', J/\psi, \dots$) and N is either the final state proton which remains intact in the interaction (elastic production) or an excited state in case of proton dissociation.

The cross section for the elastic process has been calculated by several authors. In the 'soft' pomeron picture of Donnachie-Landshoff³⁶, the photon fluctuates into a $q\bar{q}$ pair, which then interacts with the proton by exchanging a pomeron. The cross section $\sigma(\gamma p \rightarrow Vp)$ is expected to increase slowly with the γp center of mass energy W ; the exponential dependence on t , the square of the four momentum transfer at the proton vertex, is expected to become steeper as W increases (shrinkage).

In models^{37,38,39} based on perturbative QCD, the pomeron is treated as a perturbative two-gluon system: the cross section is then related to the square of the gluon density in the proton and a strong dependence of the cross section on W is expected. The prediction, taking into account the HERA measurements of the gluon density at low x_{Bjorken} , is that the cross section should have at low x a dependence of the type $W^{0.8-0.9}$. In order to be able to apply perturbative QCD, a 'hard' scale has to be present in the process. The scales involved in process (21) are the mass of the quarks in the vector meson V , the photon virtuality Q^2 and t .

In the following we summarize results on vector meson production obtained by the H1 and ZEUS Collaborations at HERA, in the energy range $W = 40 - 150$ GeV, starting from $Q^2 \simeq 0$ and increasing the scales in the process.

ⁱCombined session with Working Group 2, on Photoproduction Interactions.

We also review results at high t , which were presented for the first time at this conference. Results on vector meson production with diffractive proton dissociation events were also discussed.

3.2 Vector mesons at $Q^2 \simeq 0$

Elastic vector meson production at $Q^2 \simeq 0$ has been studied by both Collaborations^{40,41}. The cross section for $\rho, \omega, \phi, J/\psi$ production is plotted versus W in fig. 7b (from⁴⁴, where the results obtained at HERA ($W = 50 - 200$ GeV) are compared to those of fixed target experiments ($W \simeq 10$ GeV). At $Q^2 \simeq 0$, the cross section is mainly due to transversely polarized photons. The Donnachie-Landshoff model (DL), where one expects for the $\sigma(\gamma p) \rightarrow Vp$ cross section a dependence of the type $\simeq W^{0.22}$, reproduces the energy dependence for the light vector mesons (see lines in the figure). In the same way the dependence of the total photoproduction cross section is well reproduced by the soft pomeron model¹⁸ (see figure). In contrast, this model fails to describe the strong W dependence observed in the J/ψ data. Note that this steep W dependence, $\sigma(\gamma p \rightarrow Vp) \simeq W^{0.8}$, is implied even within the restricted W range covered by the HERA data alone. In this case the hard scale is provided by the charm mass.

Elastic J/ψ production is a very important process to determine the gluon density in the proton, as the cross section is proportional to the square of this density. The gluon density can be measured in the range $5 \times 10^{-4} < x \simeq \frac{(m_V^2 + Q^2 + |t|)}{W^2} < 5 \times 10^{-3}$. An improved calculation for this process was presented⁴²: although the normalization of the cross section is known theoretically with a precision of 30%, the shape of the W dependence is very sensitive to different parton density parametrizations in the proton. Open charm production is also a very sensitive probe of the gluon density, and the perturbative calculation has no ambiguities in the normalization; however it is experimentally more difficult.

3.3 Vector mesons at high Q^2

Results on vector meson production at high Q^2 have been presented by H1⁴³. The cross section for the process ($\gamma^* p \rightarrow \rho p$) with the H1 1994 data is shown in fig. 8a, together with the ZEUS 1993 results⁴⁵, in the $\gamma^* p$ centre of mass energy W of 40 to 140 GeV, and at $Q^2 = 10, 20$ GeV². At these values of Q^2 , the $\sigma(\gamma^* p \rightarrow Vp)$ cross section is dominated by longitudinally polarized photons. Comparing the H1 data to the NMC data at $W \simeq 10$ GeV, a dependence of

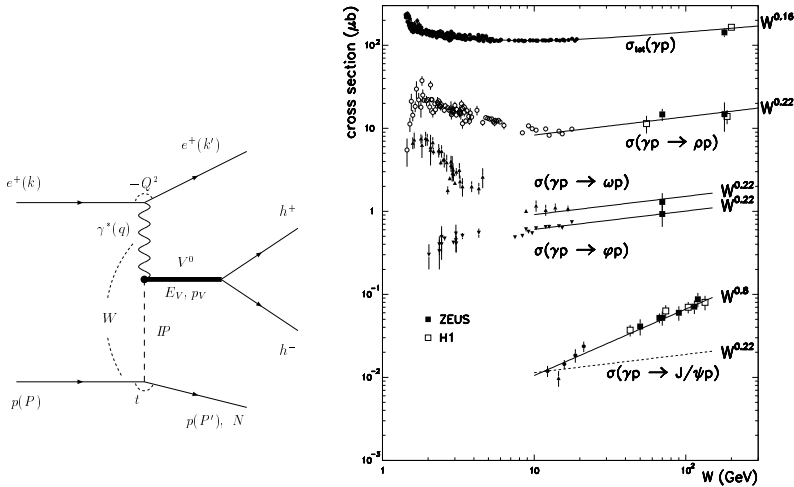


Figure 7: (a) Feynman graph of vector meson production at HERA; (b) Cross section versus W for vector meson production at $Q^2 \simeq 0, t \simeq 0$.

the type $\sigma \simeq W^{0.6}$ at $Q^2 = 10 \text{ GeV}^2$ for the the cross section is obtained. The t dependence of the reaction $\gamma^* p \rightarrow pp$ for $|t| < 0.5 \text{ GeV}^2$ is well reproduced by an an exponential distribution $\exp(-b|t|)$, with $b \simeq 7 \text{ GeV}^{-2}$ (see table 1). In the framework of Regge theory, the shrinkage of the elastic peak can be written as $b(W^2) = b(W^2 = W_0^2) + 2\alpha' \ln(W^2/W_0^2)$, where α' is the slope of the pomeron trajectory. Comparing the H1 1994 data with the NMC data, the parameter α' which is obtained is in agreement with that expected from a soft pomeron trajectory ($\alpha' = 0.25 \text{ GeV}^{-2}$). The H1 1994 and the ZEUS 1993 data are compatible within the errors, however while the H1 ρ data suggest that we are in a transition region between soft and hard processes, the ZEUS 1993 data show a stronger W dependence for the cross section when compared to NMC ($\sigma \simeq W^{0.8}$), and a flatter t distribution, $b \simeq 5 \text{ GeV}^{-2}$ (tab. 1). These two last results suggest a hard pomeron exchange. More data will allow to reduce the uncertainties due to the non resonant background, to the proton dissociation background and to study the W dependence in the region covered by the HERA data alone.

The ratio of the dissociative over elastic ρ cross section was measured⁴³ to be $0.59 \pm 0.12 \pm 0.12$, with no significant Q^2 dependence (in the range between 8 and 36 GeV^2) or W dependence (in the range between 60 and 180 GeV).

J/ψ production was presented by both collaborations^{43,46}: while the ratio of the cross sections $\sigma(J/\psi)/\sigma(\rho)$ is of the order of $10^{-3} - 10^{-2}$ at $Q^2 \simeq 0$,

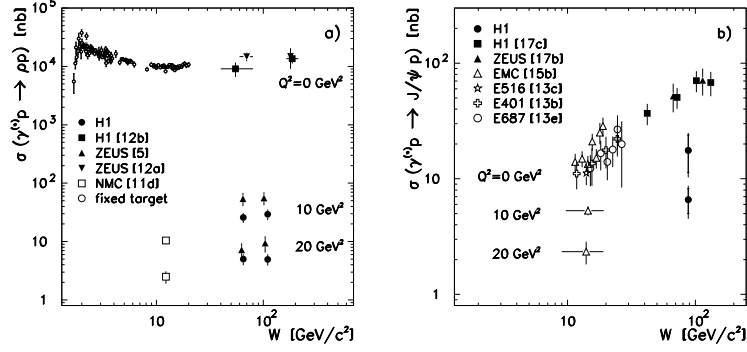


Figure 8: Cross section versus W for vector meson production at $Q^2 \simeq 0$ and at high Q^2 , for ρ (a) and J/Ψ (b) production.

this ratio becomes close to 1 at $Q^2 > 10 \text{ GeV}^2$ (see figs 8a and 8b, from ⁴⁴), as predicted by perturbative QCD ⁴⁷.

3.4 Vector mesons at high $|t|$

The installation in 1995 of a new detector ⁴⁸ in the ZEUS experiment at 44 m from the interaction point in the direction of the outgoing positron, allowed to tag the scattered positron and to access vector mesons at $Q^2 < 0.01 \text{ GeV}^2$, $1 < |t| < 4.5 \text{ GeV}^2$ and in the W range $80 < W < 100 \text{ GeV}$. About 600 ρ candidates and 80 ϕ candidates were found: from Monte Carlo studies it was seen that at $t > 1 \text{ GeV}^2$, the main contribution is proton dissociative production. The ratio of the cross sections $\sigma(\phi)/\sigma(\rho)$ was measured in two ranges of t ($1.2 < |t| < 2 \text{ GeV}^2$, $2 < |t| < 4.5 \text{ GeV}^2$), and was found to be $0.16 \pm 0.025(\text{stat.}) \pm 0.02(\text{sys.})$ and $0.18 \pm 0.05(\text{stat.}) \pm 0.04(\text{sys.})$ respectively, close to the value of $2/9$ predicted by SU(3) flavour symmetry. This value is significantly higher than the value obtained at $t \simeq 0$, $Q^2 \simeq 0$ and is instead compatible with the value obtained ^{43,49} at $Q^2 \simeq 12 \text{ GeV}^2$, suggesting that at high $|t|$ perturbative QCD plays an important role. Vector meson production at high $|t|$ has been suggested ⁵⁰ as a very nice field to study the hard pomeron, since the cross sections are calculable in pQCD.

Table 1: Results on the value b (in GeV^{-2}) fitted to the exponential t distributions for elastic and proton dissociation vector meson production at HERA. The first error is the statistical, the second error is the systematic one.

		$b(\text{H1})$	$b(\text{ZEUS})$
$Q^2 = 0, t < 0.5 \text{ GeV}^2$, elastic	ρ	$10.9 \pm 2.4 \pm 1.1$	$9.9 \pm 1.2 \pm 1.4$
$Q^2 = 0, 0.07 < t < 0.4 \text{ GeV}^2$			$9.6 \pm 0.8 \pm 1.2$ (LPS)
$Q^2 = 0, t < 0.5 \text{ GeV}^2$, elastic	ω		$10.6 \pm 1.1 \pm 1.4$
$Q^2 = 0, t < 0.5 \text{ GeV}^2$, elastic	ϕ		$7.3 \pm 1.0 \pm 0.8$
$Q^2 = 0, t < 1 \text{ GeV}^2$, elastic	J/Ψ	$4.0 \pm 0.2 \pm 0.2$	
$Q^2 \simeq 10, t < 0.5 \text{ GeV}^2$, elastic	ρ	$7.0 \pm 0.8 \pm 0.6$	$5.1^{+1.2}_{-0.9} \pm 1.0$
$Q^2 \simeq 10, t < 0.8 \text{ GeV}^2$, elastic	J/Ψ	$b = 3.8 \pm 1.2^{+2.0}_{-1.6}$	
$Q^2 = 0, 0.04 < t < 0.45 \text{ GeV}^2$, p-dissociation	ρ		$5.3 \pm 0.8 \pm 1.1$ (LPS)
$Q^2 = 10, t < 0.8 \text{ GeV}^2$, p-dissociation	ρ	$2.1 \pm 0.7 \pm 0.4$	
$Q^2 = 10, t < 1 \text{ GeV}^2$, p-dissociation	J/Ψ	$1.6 \pm 0.3 \pm 0.1$	
$Q^2 = 0, 1 < t < 4.5 \text{ GeV}^2$, p-dissociation	ρ		$\simeq 2.5$

3.5 Outlook

A summary of the t slopes presented at this conference is given in table 1. The results marked with LPS were obtained using the ZEUS Leading Proton Spectrometer⁴⁰, which detects the scattered proton and measures its momentum; the LPS allows to tag a clean sample of elastic events and to measure t directly. The parameter b is proportional, in diffractive processes, to the square of the radius of the interaction, which decreases with the mass of the quark or the photon virtuality, as confirmed by the results in the table. Note that the result in inclusive diffractive deep inelastic events obtained by the ZEUS experiment using the LPS is $b = 5.9 \pm 1.3^{+1.1}_{-0.7} \text{ GeV}^{-2}$, for a mean value of the mass of the final hadronic system of 10 GeV ¹⁵. Also results in proton dissociation events were presented at this conference. In ρ^0 photoproduction events with proton dissociation, the exponential slope is $b \simeq 5 \text{ GeV}^{-2}$ at $t \simeq 0$ ⁴⁰ and becomes flatter, $b \simeq 2.5 \text{ GeV}^{-2}$, at high $|t|$ ⁴⁸.

In summary, vector meson production at HERA is a rich field for studying the interplay between soft and hard interactions in diffractive processes. More luminosity and the forward proton spectrometers installed in both the H1 and ZEUS experiments will allow to make more precise measurements.

Acknowledgments

We wish to thank all the colleagues who participated in this parallel session, our colleagues convenors of the shared sessions, the secretariat of the session,

and the organizers and the secretariat of DIS96 for the warm hospitality. VDD would like to thank PPARC and the Travel and Research Committee of the University of Edinburgh for the support. EG wants to thank G. Barbagli, M. Arneodo and A. Levy for a careful reading of part of the manuscript.

References

1. M. Derrick et al., ZEUS Coll., *Phys. Lett. B* **315**, 1993 (481).
2. T. Ahmed et al., H1 Coll., *Nucl. Phys. B* **429**, 1994 (377).
3. H. Abramowicz, *Diffraction Hard Scattering - Report from the HERA Workshop*, in these proc.
4. A. Solano, *Monte Carlo Generators for Diffractive Processes*, in these proc.
5. J.C. Collins, J. Huston, J. Pumplin, H. Weerts and J.J. Whitmore, *Phys. Rev. D* **51**, 3182 (1995).
6. A. Berera and D.E. Soper, *Phys. Rev. D* **53**, 6162 (1996).
7. L. Trentadue and G. Veneziano, *Phys. Lett. B* **323**, 201 (1994);
L. Trentadue, *Fracture Functions*, in these proc.
8. G. Ingelman and P.E. Schlein, *Phys. Lett. B* **152**, 256 (1985).
9. A. Donnachie and P.V. Landshoff, *Phys. Lett. B* **191**, 309 (1987); *Nucl. Phys. B* **303**, 634 (1988).
10. A. Donnachie and P.V. Landshoff, *Nucl. Phys. B* **244**, 322 (1984).
11. L. Jenkovszky, *Diffraction Deep Inelastic Scattering with a Logarithmic Pomeron Trajectory*, in these proc.
12. T. Ahmed et al., H1 Coll., *Phys. Lett. B* **348**, 681 (1995).
13. M. Derrick et al., ZEUS Coll., *Z. Phys. C* **68**, 569 (1995).
14. H. Kowalski, ZEUS Coll., *Measurement of the Diffractive Cross Section in Deep Inelastic Scattering*, in these proc.;
M. Derrick et al., ZEUS Coll., *Z. Phys. C* **70**, 391 (1996).
15. E. Barberis, ZEUS Coll., *Deep Inelastic Diffractive Results with the ZEUS Leading Proton Spectrometer*, in these proc.
16. P.R. Newman, H1 Coll., *Inclusive Measurements of Diffraction in Deep Inelastic Scattering and Photoproduction at HERA*, in these proc. and preprint DESY 96-162.
17. N.N. Nikolaev, *Diffractive DIS from the Colour Dipole BFKL Pomeron*, in these proceedings;
N.N. Nikolaev and B. Zakharov, *Z. Phys. C* **53**, 331 (1992).
18. P.V. Landshoff, *The Soft Pomeron*, in these proc.
19. A. Mehta, H1 Coll., *New Results on Diffractive Deep Inelastic Scattering*, invited talk at the Topical Conf. on Hard Diffraction, Eilat, 1996.

20. E. Predazzi, *Odd C-parity effects in diffractive physics*, in these proc.
21. W.J. Stirling, $F_2^D/F_2(\text{pomeron})$, in these proc.
22. L. Frankfurt and M. Strikman, *Phys. Rev. Lett.* **64**, 1914 (1989);
J.C. Collins, L. Frankfurt and M. Strikman, *Phys. Lett. B* **307**, 161 (1993);
A. Berera and D.E. Soper, *Phys. Rev. D* **50**, 4328 (1994).
23. J. Theissen, H1 Coll., *Jets in Diffractive ep Scattering*, in these proc. and preprint DESY 96-162.
24. S. Tapprogge, H1 Coll., *Energy Flow and Open Charm Production in Diffractive Deep-Inelastic Scattering*, in these proc. and preprint DESY 96-162.
25. A. Valkarova, H1 Coll., *Thrust Jet Analysis of Diffractive Deep-Inelastic Scattering Events at HERA*, in these proc. and preprint DESY 96-162.
26. A. Berera, *Diffractive Factorization - A Simple Field Theory Model for $F_2^D(\beta x_P, Q^2, x_P, t)$* , in these proc.
27. J. Bartels, *Diquark jets in DIS diffractive dissociation*, in these proc.
28. M. Derrick *et al.*, ZEUS Coll., *Phys. Lett. B* **356**, 129 (1995).
29. H. Jung, *Comp. Phys. Commun.* **86**, 147 (1995).
30. W. Buchmüller, *Phys. Lett. B* **353**, 335 (1995);
W. Buchmüller and A. Hebecker, *Phys. Lett. B* **355**, 573 (1995).
31. T. Gehrmann and W.J. Stirling, *Z. Phys. C* **70**, 89 (1996).
32. T. Arens, M. Diehl, P.V. Landshoff and O. Nachtmann, *Some Tests for the Helicity Structure of the Pomeron in ep Collisions*, preprint HD-THEP-96-06.
33. F. Zarnecki, ZEUS Coll., *Diffractive in Charged Current DIS*, in these proc.
34. J.F. Martin, ZEUS Coll., *Observation of High Energy Forward Neutrons in Deep Inelastic Scattering*, in these proc.
35. W. Wittek, E665 Coll., *Recent Results on Diffractive Scattering in Muon-Proton Interactions from the E665 Experiment*, in these proc.
36. A. Donnachie and P.V. Landshoff, *Phys. Lett. B* **296**, 227 (1992).
37. M.G. Ryskin, *Z. Phys. C* **57**, 89 (1993).
38. S.J. Brodsky *et al.*, *Phys. Rev. D* **50**, 3134 (1994).
39. J. Nemchik *et al.*, *Phys. Lett. B* **341**, 228 (1994).
40. R. Sacchi, ZEUS Coll., *Photoproduction of ρ , ω and ϕ Mesons at ZEUS*, in these proc., and ref. therein.
41. S. Schiek, G. Schmidt, H1 Coll., *Photoproduction of Vector Mesons at H1*, in these proc. and preprint DESY 96-162, and ref. therein.
42. A.D. Martin, *Diffractive Production of $c\bar{c}$ Systems at HERA*, in these proc.

43. B. Clerbaux, H1 Coll., *Vector Meson Production at High Q^2* , in these proc. and preprint DESY 96-162, and ref. therein.
44. S. Aid *et al.*, H1 Coll., NPB **468**, 1996 (3).
45. M.Derrick *et al.*, ZEUS Coll., *Phys. Lett. B* **356**, 601 (1995).
46. L. Stanco, ZEUS Coll., *J/ψ production at HERA*, in these proc.
47. H. Abramowicz, L. Frankfurt and M. Strikman, *Interplay of Hard and Soft Physics in Small x Deep Inelastic Processes*, preprint DESY 95-047 (1995).
48. K. Piotrkowski, ZEUS Coll., *Diffraction Photoproduction of ρ and ϕ at large $|t|$* , in these proc.
49. M. Derrick *et al.*, ZEUS Coll., *Measurement of the Reaction $\gamma^*p \rightarrow \phi p$ in Deep Inelastic e^+p Scattering at HERA*, preprint DESY 96-067 (1996).
50. D.Yu. Ivanov, *Diffraction Light Vector Meson Production at Large Momentum Transfer*, in these proc.